The *Drosophila* Ste20 family kinase dMST functions as a tumor suppressor by restricting cell proliferation and promoting apoptosis

Jianhang Jia,[1] Wensheng Zhang,[1] Bing Wang,[1] Richard Trinko,[2] and Jin Jiang[1,3]

[1]Center for Developmental Biology and Department of Pharmacology and [2]DCMB program, University of Texas Southwestern Medical Center, Dallas, Texas 75390-9133, USA

In a genetic screen for mutations that restrict cell growth and organ size, we identified a new tumor suppressor gene, *dMST*, which encodes the *Drosophila* homolog of the mammalian Ste20 kinase family members MST1 and MST2. Loss-of-function mutations in *dMST* result in overgrown tissues containing more cells of normal size. *dMST* mutant cells exhibit elevated levels of Cyclin E and DIAP1, increased cell growth and proliferation, and impaired apoptosis. dMST forms a complex with Sav and Wts, two tumor suppressors also implicated in regulating both cell proliferation and apoptosis, suggesting that they act in common pathways.

Received July 16, 2003; revised version accepted August 25, 2003.

In animal development, cell number and organ size are tightly controlled by mechanisms that regulate cell proliferation and cell death. Deregulation of these mechanisms has been implicated in cancers (Hanahan and Weinberg 2000). Although many genes controlling either cell proliferation or cell death have been identified, few genes have been implicated in regulating both processes. One exception is the pathway defined by the two genes *salvador* (*sav*) and *warts* (*wts*)/*large tumors* (*lats*), which encode WW domain-containing protein and Ser/Thr kinase, respectively (Justice et al. 1995; Xu et al. 1995; Tapon et al. 2002). Mosaic animals carrying *sav* or *wts* mutant clones exhibit tissue overgrowth phenotypes. Both *sav* and *lats* mutant cells contain elevated levels of Cyclin E and *Drosophila* inhibitor of apoptosis 1 (DIAP1), leading to increased cell proliferation and impaired apoptosis (Tapon et al. 2002). Sav binds Wts in vitro, and they genetically interact, suggesting they act in a common pathway to regulate cell proliferation and cell death. How the *sav/wts* pathway is regulated and the mechanisms by which it controls cell proliferation and apoptosis are not known.

[*Keywords*: dMST; MST1; tumor suppressor; apoptosis; Wts; Sav]
[3]Corresponding author.
E-MAIL jin.jiang@utsouthwestern.edu; FAX (214) 648-1960.
Article and publication are at http://www.genesdev.org/cgi/doi/10.1101/gad.1134003.

Results and Discussion

To identify novel tumor suppressor genes, we systematically screened the *Drosophila* genome for mutations that cause tissue overgrowth phenotypes (see Materials and Methods). From this screen, we identified three alleles of a gene we named *dMST* (*Drosophila* homolog of MST1 and MST2). We used $dMST^{BF33}$ for most analyses described in this study, as the molecular nature of $dMST^{BF33}$ suggests that it is likely to be a null allele (see below).

dMST *mutations result in tumor-like growth*

Compared with wild-type eyes, *dMST* mosaic eyes are significantly larger and often protrude out in folds (Fig. 1A,B). Tumorous outgrowths were also observed when *dMST* clones were induced in other places, including the thorax, wing, and haltere (Fig. 1C–G). Hence, *dMST* is generally required for restricting tissue growth and organ size.

To determine how *dMST* controls organ size, we generated labeled *dMST* clones in wing discs and compared cell size and clone size between mutant clones and twin spots. *dMST* mutant cells do not exhibit discernible changes in cell size (Fig. 1J–K′). Moreover, *dMST* mutant cells differentiated into wing margin bristles of normal size (Fig. 1H). However, *dMST* clones occupy significantly larger areas and contain more cells than do wild-type twin spots (Fig. 1I,I′). As mutant clones and twin spots were derived from mitotic sister cells born at the same developmental stages, the increase in cell numbers and tissue mass of *dMST* mutant clones over twin spots suggests that *dMST* mutant cells grow and proliferate faster than do wild-type cells. Hence, the increase in size of *dMST* mosaic organs is caused by an increase in cell number but not cell size.

dMST *regulates both cell proliferation and apoptosis*

To further explore cell proliferation defects caused by *dMST* mutations, we focused on eye development. In wild-type eye discs, a single stripe of cells, referred to as the second mitotic wave (SMW), enters S phase synchronously posterior to the morphogenetic furrow (MF), and little bromodeoxyuridine (BrdU) labeling is present posterior to the SMW (Fig. 2A; Wolff and Ready 1993). In contrast, *dMST* mosaic discs exhibit extensive BrdU incorporation posterior to the SMW (Fig. 2B). To determine if extra mitosis also occurs in *dMST* mutant eye discs, we used the anti-phosphohistone H3 (pH3) antibody to label cells in M phase. In wild-type eye discs, few cells posterior to the SMW exhibit pH3 staining (Fig. 2C). In contrast, *dMST* mutant discs contain increased number of cells in M phase posterior to the SMW (Fig. 2D), suggesting that *dMST* mutations increase cell proliferation.

Cyclin E is an important regulator of S-phase initiation and progression in imaginal disc development (Richardson et al. 1995). In wild-type discs, Cyclin E is up-regulated at the SMW (Fig. 2E). We found that *dMST* mutant clones accumulate high levels of Cyclin E in a cell-autonomous fashion (Fig. 2F–F″), which is consistent with the increased cell proliferation in *dMST* mutant discs.

In wild-type eyes, excessive cells between differentiated ommatidias are eliminated by a wave of apoptosis at

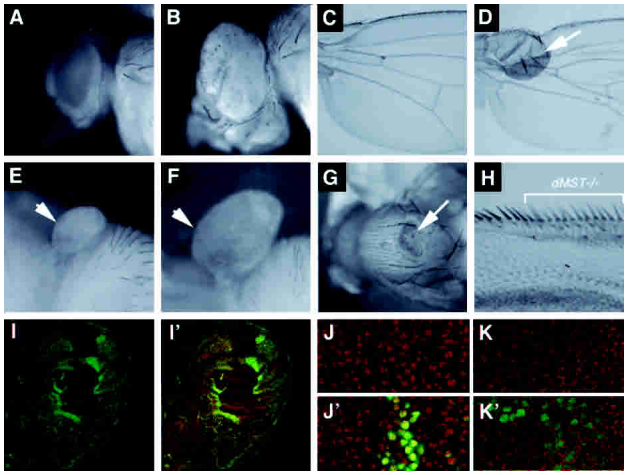

Figure 1. *dMST* mutations result in tumorous overgrowths. (*A*,*B*) Adult eyes of wild type (*A*) or containing *dMST* mutant clones (*B*). (*B*) *dMST* mosaic eye is enlarged and protrudes out in folds. (*C*,*D*) A wild-type wing (*C*) or a wing containing a *dMST* clone located near the wing hinge (arrow in *D*). (*E*,*F*) A control (*E*) and a *dMST* mosaic haltere (*F*). (*G*) A *dMST* mutant clone on the thorax exhibits tumor-like growth (arrow). (*H*) High-magnification view of wing margin containing *dMST* mutant clones labeled by *y*– (indicated by the bracket). *dMST* mutant cells differentiate into margin bristles of normal size. (*I*,*I*′) A late third instar wing disc containing *dMST* clones stained with a nuclear dye, 7-AAD (red in *I*′) and anti-Myc antibody (green in *I*,*I*′). *dMST* mutant clones lack *hs-Myc-GFP* expression, whereas the twin spots exhibit enhanced *hs-Myc-GFP* expression. (*J*–*K*′) High-magnification view of *dMST* mutant clones and twin spots labeled with 7-AAD (red in *J*,*J*′), which labels the nuclei, or anti-Armadillo (Arm) antibody (red in *K*,*K*′), which stains cell membrane. *dMST* mutant cells are recognized by the lack of Myc-GFP expression (green). *dMST* mutant cells are of the normal size compared with wild-type cells.

early pupal stage so that a single layer of cells exists between two adjacent ommatidias (Fig. 2G; Wolff and Ready 1993). In contrast, the *dMST* mutant disc contains multiple layer interommatidial cells (Fig. 2H). The persistence of excessive interommatidial cells in *dMST* mutant discs implies that apoptosis could be compromised. To test this, we examined cell death in wild-type and *dMST* mosaic pupal retina 38 h after pupa formation (APF) and found that apoptosis was diminished in *dMST* mutant cells (Fig. 2I–I″). Hence, *dMST* is required for apoptosis during development.

In *Drosophila*, apoptosis is triggered by death inducers, including *head involution defective* (*hid*; Abrams 1999). Expressing *GMR-hid* induces precocious cell death in larval eye discs (Fig. 2J), which is blocked in *dMST* mutant cells (Fig. 2K,K′). As a consequence, adult eyes derived from *GMR-hid*-expressing discs that also contain *dMST* mutant clones are larger than those derived from wild-type discs expressing *GMR-hid* (Fig. 2L,M). In *Drosophila*, death promoters induce apoptosis in part by down-regulating the levels of the death inhibitor DIAP1 (Ryoo et al. 2002; Yoo et al. 2002). We found that *dMST* mutant cells exhibit higher levels of DIAP1 than do wild-type cells (Fig. 2N–O′), suggesting that *dMST* promotes cell death at least in part by down-regulating the levels of DIAP1. We also found that the expression of a *diap1-lacZ* reporter gene is elevated in *dMST* mutant cells (Fig. 2Q,Q′), indicating that *dMST* inhibits the transcription of *diap1*.

Molecular cloning of dMST

The *dMST* mutations were mapped by high-resolution meiotic recombination (Fig. 3A; see Materials and Methods). We sequenced several candidate genes for molecular lesions present in mutagenized chromosomes containing *dMST* alleles. Both $dMST^{JM1}$ and $dMST^{BF33}$ in-

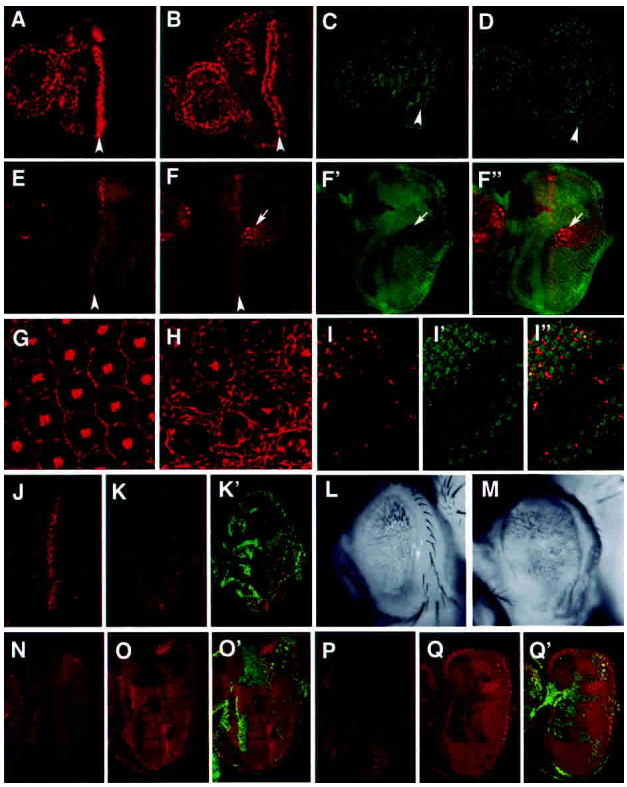

Figure 2. *dMST* controls both cell proliferation and apoptosis. (*A*–*D*) BrdU incorporation (*A*,*B*) or phospho-H3 staining (*C*,*D*) of wild-type eye discs (*A*,*C*) or *dMST* mosaic eye discs (*B*,*D*). Arrowheads indicate the second mitotic wave (SMW). All eye discs are oriented with anterior to the left. (*B*,*D*) *dMST* mosaic discs exhibit extensive BrdU incorporation and increased phospho-H3-positive cells posterior to the SMW. (*E*) Cyclin E expression in wild type. (*F*–*F*″) Cyclin E expression in *dMST* mosaic discs. *dMST* mutant cells are labeled by the lack of Myc-GFP expression (green). *dMST* mutant cells posterior to the SMW accumulate high levels of Cyclin E cell autonomously (arrows). (*G*,*H*) Phalloidin staining of wild type (*G*) or *dMST* mosaic (*H*) pupal eye disc (46 h APF). (*G*) The wild-type pupal eye disc contains a single layer of interommatidial cells. (*H*) In contrast, the *dMST* mutant disc contains multiple layers of interommatidial cells. (*I*–*I*″) A *dMST* mosaic pupal eye disc (38 h APF) doubly stained to show TUNEL (red) and Myc-GFP (green) expression. *dMST* mutant cells are labeled by the lack of green staining. The TUNEL staining is confined to wild-type cells. (*J*) A late third eye disc expressing *GMR-hid* and stained with an antibody against an activated form of the *Drosophila* caspase Drice (Drice-Act), which labels dying cells (Yoo et al. 2002). Expression of *GMR-hid* induces precocious cell death. (*K*,*K*′) A *dMST* mosaic eye disc expressing *GMR-hid* stained with antibodies against Drice-Act (red) and Myc (green). *dMST* mutant cells are recognized by the lack of green staining. Ectopic cell death induced by *GMR-hid* is blocked in *dMST* mutant cells. (*L*,*M*) Adult eyes derived from *GMR-hid*-expressing discs (*L*) or *dMST* mosaic discs expressing *GMR-hid* (*M*). (*N*–*Q*) Diap1 protein accumulation (red in *N*–*O*′) or *diap1-lacZ* expression (red in *P*–*Q*′) in wild-type (*N*,*P*) or *dMST* mosaic (*O*,*O*′,*Q*,*Q*′) eye discs. *dMST* mutant cells, which lack Myc-GFP expression (green), exhibit high levels of DIAP1 protein (*O*,*O*′) and *diap1-lacZ* expression (*Q*,*Q*′).

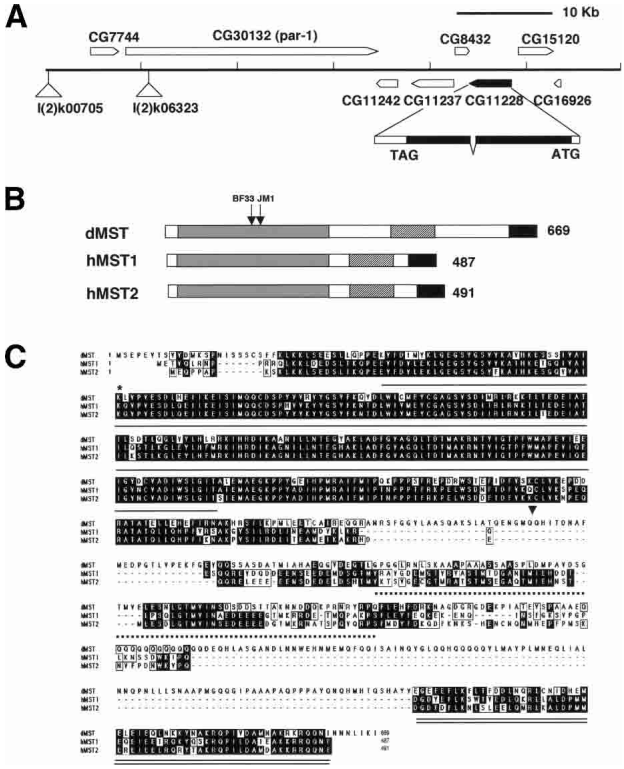

Figure 3. *dMST* encodes the homolog of the mammalian Ste20-like kinases MST1 and MST2. (*A*) The genomic region of the *dMST* locus. The positions of two of the P-element insertions used for mapping—*l(2)k06323* and *l(2)k00705*—are indicated. (*B*) Functional domains of dMST, and human MST1 (hMST1) and MST2 (hMST2). The kinase domains are shaded in gray. The black and hatched boxes indicate the dimerization and kinase inhibitory domains, respectively. The arrows indicate the positions of $dMST^{BF33}$ and $dMST^{JM1}$ mutations. (*C*) Sequence alignment among dMST, hMST1, and hMST2. The kinase domain, kinase inhibitory domain, and dimerization domain are underlined by a single solid line, a broken line, and a double solid line, respectively. The asterisk indicates K71, which is changed to R in dMSTnK>R mutant. The arrowhead marks the boundary between dMSTn and dMSTc.

troduced point mutations in the open reading frame (ORF) of an annotated gene *CG11228*, which encodes the *Drosophila* homolog of mammalian Ste20 kinase family members MST1 and MST2 (Creasy and Chernoff 1995a,b). A full-length cDNA corresponding to *CG11228* was placed under the control of a *tubulinα1* promoter to generate *tub-dMSTf*. Both $dMST^{JM1}$ and $dMST^{BF33}$ homozygotes expressing one copy of *tub-dMSTf* are viable, morphologically normal, and fertile, demonstrating that *CG11228* is *dMST*. $dMST^{JM1}$ introduced a single amino acid substitution at a conserved residue (G181E), whereas $dMST^{BF33}$ introduced a stop codon at amino acid 174 (Fig. 3B), suggesting that $dMST^{BF33}$ is likely to be a null allele.

Like its mammalian counterparts, dMST contains an N-terminally situated kinase domain and C-terminally located regulatory domains (Fig. 3B,C). The dMST kinase domain exhibits 84% and 83% identity to that of hMST1 and dMST2, respectively. The C-terminally situated dimerization and kinase inhibitory domains present in MST1 and MST2 (Creasy et al. 1996) are also highly conserved in dMST (Fig. 3C).

dMST *interacts with Sav and Wts*

The *dMST* mutant phenotypes closely resemble those caused by *sav* or *wts* mutations (see Fig. 5I,I′,L–L″,O–O″, below; Tapon et al. 2002; data not shown). It has been shown that Sav and Wts physically and genetically interact, suggesting that they may act in common pathways (Tapon et al. 2002). To determine if dMST could act in the same pathways, we examined if it physically interacts with Sav and Wts by using coimmunoprecipitation assay. We first determined if dMST binds Sav. S2 cells were transfected with DNA constructs expressing HA-tagged Sav and Flag-tagged full-length dMST (dMSTf), its N-terminal fragment containing the kinase domain (dMSTn), or its C-terminal fragment containing the regulatory domains (dMSTc; Fig. 4A). As shown in Figure 4B, both dMSTf and dMSTc, but not dMSTn, were coimmunoprecipitated with Sav, suggesting that dMST binds Sav through its C-terminal regulatory region. The dimerization domain at the C terminus of dMST appears to be essential for interaction as deletion of this domain from dMSTc abolished its ability to bind Sav (data not shown).

To define the domain in Sav that binds dMST, we gen-

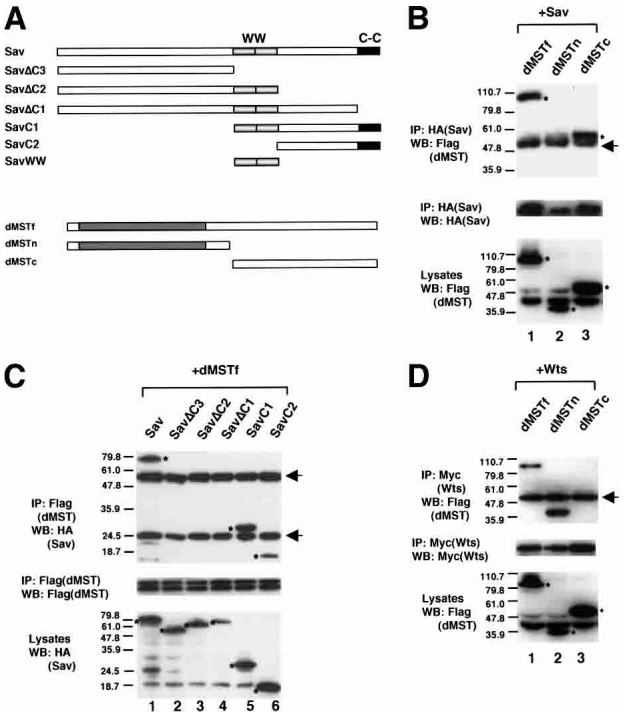

Figure 4. dMST interacts with Sav and Wts. (*A*) Schematic drawing of Sav and dMST constructs used for transfection. The WW and coiled-coil (C-C) domains of Sav are indicated by shaded and black boxes, respectively. The Sav constructs contain two copies of HA tag, whereas the dMST constructs have a Flag tag at the N terminus. (*B–D*) S2 cells were transfected in indicated DNA constructs. (*Top* and *middle* panels) Cell extracts were immunoprecipitated (IP) with indicated antibodies, followed by Western blot (WB) with corresponding antibodies, as indicated. (*Bottom* panels) Cell lysates were also directly subjected to Western blot with indicated antibodies to determine the expression levels of individual constructs. The Wts construct contains six copies of Myc tag at the N terminus. The asterisks indicate the positions of proteins expressed from the transfected constructs (*bottom* panels) or coimmunoprecipitated proteins (*top* panels). The arrows indicate immunoglobin G. Of note, dMSTf and dMSTc appear to be much larger than their predicted sizes.

erated a series of truncated forms of Sav (Fig. 4A). Both C-terminal fragments, SavC1 and SavC2, bind dMST. In contrast, all the C-terminally truncated fragments, including SavΔC1, SavΔC2, and SavΔC3, fail to bind dMST (Fig. 4C), suggesting that dMST binds the C-terminal region of Sav and the coiled-coil domain of Sav is essential.

We next examined if dMST binds Wts. S2 cells were transfected with DNA constructs expressing Myc-tagged Wts and Flag-tagged dMSTf, dMSTn, or dMSTc. As shown in Figure 4D, Wts binds dMSTf and dMSTn, but not dMSTc, suggesting that Wts interacts with the N-terminal region of dMST. The interaction between Wts and dMST is not affected by Sav, as coexpression of Sav does not increase the amount of dMSTf coimmunoprecipitated with Wts (data not shown). However, it remains possible that Sav might regulate dMST/Wts interaction in vivo at physiological concentration. Taken together, these results suggest that dMST, Wts, and Sav form a complex in which Wts and Sav bind the kinase and regulatory domains of dMST, respectively.

When overexpressed in larval eye discs by using the *GMR-gal4* driver, dMSTn, but not its kinase dead form (dMSTnK>R), induced ectopic apoptosis (Fig. 5E,F), leading to the formation of small rough eyes (Fig. 5B). Although expressing *GMR-Wts* alone does not cause any significant defect (Fig. 5C), coexpressing *GMR-Wts* with dMSTn enhanced the defects caused by expressing dMSTn alone. For example, although flies expressing *GMR-Gal4/dMSTn* are viable, coexpressing *GMR-Wts* with *GMR-gal4/dMSTn* causes flies to die as pharate adults that have smaller eyes than those of flies expressing *GMR-gal4/dMSTn* alone (Fig. 5D). Similar phenotypic enhancement was obtained when two copies of *UAS-dMSTn* were expressed under *GMR-gal4* (data not shown). In contrast, the defects caused by dMSTn are not enhanced by *GMR-Sav* (data not shown). These genetic interactions are consistent with our findings that dMSTn binds Wts but not Sav.

To determine the genetic epistasis, we overexpressed dMSTn with *GMR-gal4* in eye discs that contain *wts* or *sav* mutant clones. dMSTn induces ectopic Drice activation in *sav* mutant cells, as in the case of wild-type cells (Fig. 5G,G′). In contrast, the ectopic Drice activation induced by dMSTn is diminished in *wts* mutant cells (Fig. 5H,H′). Consistently, dMSTn blocks the up-regulation of DIAP1 in *sav*, but not in *wts*, mutant cells (Fig. 5J–K′). In addition, we found that dMSTn blocks the up-regulation of Cyclin E in *sav* but not in *wts* mutant cells (Fig. 5M′;M″,P–P″). These results suggest that dMST acts downstream of *sav* but upstream of or in parallel with *wts* to restrict cell proliferation and promote apoptosis.

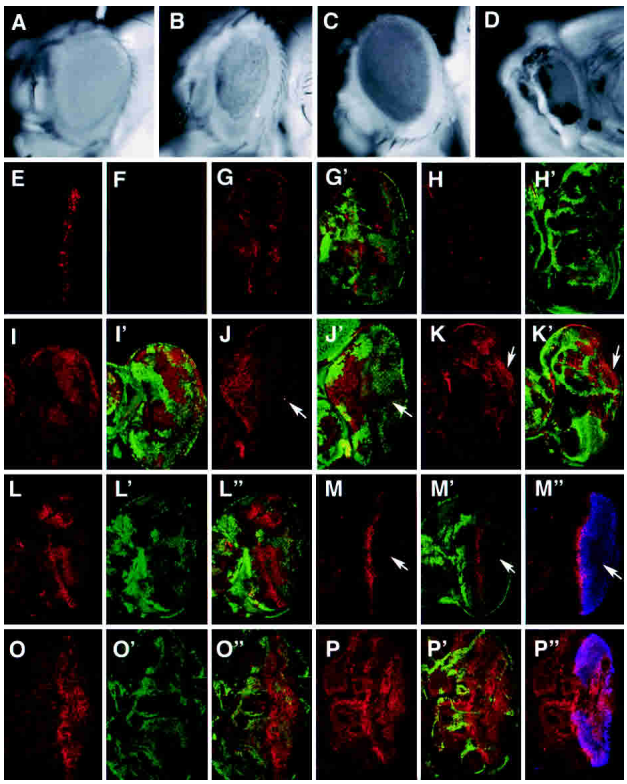

Figure 5. Genetic interaction among *dMST*, *sav*, and *wts*. (*A–D*) Adult eyes of wild type (*A*), *GMR-gal4/UAS-dMSTn* (*B*), *GMR-Wts* (*C*), and *GMR-gal4/UAS-dMSTn;GMR-Wts* (*D*). (*E,F*) Drice-Act staining in eye discs expressing *GMR-gal4/UAS-dMSTn* (*E*) or *GMR-gal4/UAS-dMSTnKR* (*F*). (*G–H′*) Drice-Act staining (red) in eye discs expressing *GMR-gal4/UAS-dMSTn* and containing *sav* (*G,G′*) or *wts* (*H,H′*) mutant clones. *sav* or *wts* mutant cells are labeled by the lack of Myc-GFP staining (green). (*I–J′*) DIAP1 expression (red) in *sav* mosaic eye disc (*I,I′*) or *sav* mosaic eye disc expressing *GMR-gal4/UAS-dMSTn* (*J,J′*). *sav* mutant cells are labeled by the lack of Myc-GFP staining (green). dMSTn blocks the up-regulation of DIAP in *sav* mutant cells (arrow). (*K,K′*) DIAP1 expression in *wts* mosaic disc expressing *GMR-gal4/UAS-dMSTn*. *wts* mutant cells (labeled by the lack of green staining) exhibit high levels of DIAP1 even though they express *GMR-gal4/UAS-dMSTn* (arrow). (*L–P″*) Cyclin E staining (red) in *sav* (*L–L″*), *wts* (*O–O″*) mosaic discs, or *sav* mosaic disc expressing *GMR-gal4/UAS-dMSTn* (*M–M″*), or mosaic disc expressing *GMR-gal4/UAS-dMSTn* (*P–P″*). *sav* and *wts* mutant cells are labeled by the lack of Myc-GFP staining (green). dMSTn expression is indicated by Flag staining (blue). *sav* mutant cells accumulate high levels of Cyclin E cell autonomously (*L–L″*), which is suppressed by dMSTn (arrows in *M–M″*). (*P–P″*) In contrast, *wts* mutant cells accumulate high levels of Cyclin E even though they express dMSTn.

Conclusion and perspective

The MST subfamily of Ser/Thr kinases is classified as putative mitogen-activated protein kinase kinase kinase kinase (MAP4K; Dan et al. 2001). Although numerous studies have been carried out to address their biochemical properties and regulations in cultured cells (Creasy and Chernoff 1995b; Creasy et al. 1996; Hirai et al. 1997; Graves et al. 1998; Lee et al. 1998; Glantschnig et al. 2002; Lee and Yonehara 2002; Cheung et al. 2003), their physiological roles remain elusive. In this study, we demonstrated that dMST plays a pivotal role in controlling cell number and organ size in *Drosophila* development. We showed that dMST fulfills such a role both by restricting cell growth and proliferation and by promoting cell death. The cell-autonomous elevation of Cyclin E and DIAP1 levels in *dMST* mutant clones suggest that dMST regulates cell proliferation and cell death cell autonomously. We provide biochemical evidence that dMST, Sav, and Wts form a complex. Our genetic epitasis study suggests *sav* acts upstream of dMST whereas *wts* downstream of or in parallel with dMST. Sav could regulate the formation or activity of dMST/Wts kinase complex. Alternatively, Sav could act to bridge the dMST/Wts kinase complex to its substrates, a function that can be bypassed by excess amounts of dMSTn.

It should be noted that *sav*, *dMST*, and *wts* may not

simply act in a linear pathway, as *wts* mutant phenotypes appear to be more severe than those caused by *sav* or *dMST* mutations (data not shown). In addition, *sav wts* double-mutant phenotypes are stronger than *sav* or *wts* single-mutant phenotypes (Tapon et al. 2002). Hence, although our results suggest that dMST, Sav, and Wts act in common pathways, they may exist in multiple complexes and have independent functions.

It has been shown that human Sav is mutated in several cancer cell lines, and mice lacking a homolog of *wts/lats* develop hyperplasia and tumors in several tissues (St. John et al. 1999; Tapon et al. 2002), raising the possibility that mammalian MST1 and MST2 may also function as tumor suppressors. In support of this notion, MST1 and MST2 have been implicated in promoting cell death in cultured mammalian cells (Graves et al. 1998; Lee et al. 2001; Cheung et al. 2003). It remains to be determined whether MST1 and MST2 also regulate cell proliferation in mammals. Given the functional conservation between many insect and mammalian pathways, we speculate that the mammalian MST/Sav/Lats pathway may also participate in restricting cell number and organ size during normal development, and its malfunction may lead to cancers.

Materials and methods

Mutations and transgenes

The scheme for genetic screen using the *eyFLP* system has been described (Newsome et al. 2000; Amanai and Jiang 2001). For 2R and 3R screen, isogenic *FRT*-containing males (*FRT42D* and *FRT82B*) were mutagenized with 25 mM ethylmethanesulfonate (EMS). After 24 h recovery, the males were mated with female virgins with corresponding *eyFLP/FRT* (y w *eyFLP2; FRT42D w+ l[2] cl-R1/Cyo [y+]* for 2R or *y w eyFLP2 glass-lacZ; FRT82B w+ cl3R3/TM6B, y+* for 3R). The F_1 progenies exhibiting enlarged eyes were back-crossed to the *eyFLP/FLP* stocks for verifying the phenotypes and germline transmission. The F_2 progenies that retained the overgrowth phenotypes were crossed to the balancer stock, *y w; Sp/Cyo[y+]; TM2/TM6B* to establish lines. Three alleles of *dMST* (*dMST$^{l\!M1}$*, *dMST$^{l\!M4}$*, and *dMST^{BF33}*), two alleles of *sav* (*sav^{SH8}* and *sav^{SH13}*), and three alleles of *wts* (*wts^{R23}*, *wts^{SH15}*, and *wts^{SH16}*) were isolated. By using a combination of meiotic recombination and complementation test with the 2R deficiency kit, *dMST* mutations were mapped to a gap (56C11–56F5) between two nonoverlapping deficiencies *Df(2R)P34* (55E2–56C11) and *Df(2R)017* (56F5–56F15). Fine mapping was achieved by high-resolution meiotic recombination by using several P-element insertion lines in this region. Specifically, *dMST* is 0.062% (8/12898) distal to *l(2)k06323* (BS#10615), 0.059% (10/17011) distal to *l(2)k00705* (BS#10485), and 0.072% (12/16488) distal to *l(2)k06121* (BS#10607). *dMST* is placed distal to *l(2) k06323* and *l(2)k06121* because the majority of the recombinant chromosomes between *dMST* and the P elements retained *FRT42D*. Several candidate genes situated 30–100 kb distal to *l(2)k06323* insertion site were chosen for sequencing. *dMST* alleles were balanced over a GFP balancer. Both *dMST$^{l\!M1}$* and *dMST^{BF33}* homozygotes die at early larval stages. Genomic DNA was prepared from homozygous embryos and amplified by PCR, followed by direct sequencing. Both *dMST$^{l\!M1}$* and *dMST^{BF33}*, but not *dMST$^{l\!M4}$*, contained a point mutation in the coding region of *CG11228* (Fig. 3).

dMST full-length cDNA was obtained from Research Genetics (GH10354) and was verified by sequencing. The coding sequence for the full-length, the N-terminal fragment (1–342 amino acids), or the C-terminal fragment (343–669 amino acids) of dMST was PCR-amplified and subcloned into the *pUAST-Flag* vector to generate *UAS-dMSTf*, *UAS-dMSTn*, and *UAS-dMSTc*. All constructs contain a Flag tag fused in frame to the N terminus. *UAS-dMSTnKR* contains a single amino acid substitution at position 71 (K71R) generated by PCR-based site-direct mutagenesis. *tub-dMST* contains a 2.6-kb *tubulinα1* promoter fused to dMST full-length cDNA in Casper vector (Basler and Struhl 1994). *sav* full-length cDNA was obtained from Research Genetics (SD10307). The coding sequence corresponding to various regions of Sav was PCR-amplified and fused in frame with two copies of HA tags, followed by subcloning into the *pUAST* vector to generate *UAS-HA-Sav* (amino acids 1–608), *UAS-HA-SavC1* (amino acids 439–608), *UAS-HA-SavC2* (amino acids 507–608), *UAS-HASavWW* (amino acids 440–506), *UAST-HA-SavΔC1* (amino acids 1–591), *UAST-HA-SavΔC2* (amino acids 1–507), and *UAST-HA-SavΔC3* (amino acids 1–439). *UAS-Myc-Wts* contains six copies of Myc tag at the N terminus of Wts. Other transgenes and stocks used in this study are *diap-lacZ* (*th^{i5c8}*; Ryoo et al. 2002), *hs-Myc-GFP* (Jiang and Struhl 1998), *hs-CD2* (Jiang and Struhl 1995), *GMR-Gal4* (Freeman 1996), *GMR-hid* (Stowers and Schwarz 1999), *GMR-sav*, and *GMR-wts* (Tapon et al. 2002). *sav^{4}* is a strong allele (Tapon et al. 2002). *wts^{M72}* is a strong allele isolated in a previous screen using the *hsFLP/FRT* system (Jiang and Struhl 1995).

Generation of clones of mutant cells

dMST mutant clones were generated using FLP/FRT-mediated mitotic recombination as described previously (Jiang and Struhl 1995). The genotypes for generating *dMST* mosaic eyes with *ey-FLP*: *eyFLP2/+ or Y; FRT42D w+ l(2) cl-R1/FRT42D dMST*, or *eyFLP2/+ or Y; FRT42D hs-Myc-GFP/FRT42D dMST*. The genotype for generating *dMST* clones with *hs-FLP*: *hs-flp122/+ or Y; FRT42D hs-Myc-GFP/FRT42D dMST* or *hs-flp122/+ or Y; FRT42D hs-CD2 y+/FRT42D dMST*. For generating *dMST* mutant eyes expressing *hid*, the following genotype is used: *eye-flp/GMR-hid; FRT42D hs-Myc-GFP/FRT42D dMST*. To generate *sav* or *wts* mosaic eyes with dMSTn expression, the following genotypes were used: *eye-flp/+ or Y; GMR-hid/UAS-dMSTn; FRT82B hs-Myc-GFP/FRT82B sav^{4} (wts^{M72})*.

Immunohistochemistry

Standard protocols for immunofluorescence staining, phalloidin staining, BrdU labeling, and TUNEL assay were used (Jiang and Struhl 1998; Wolff 2000). Primary antibodies used in this study are rat anti-CycE (Richardson et al. 1995), mouse anti-phosphohistone H3 (Upstate Biotechnology), mouse and rabbit anti-Diap1 (Ryoo et al. 2002; Yoo et al. 2002), rabbit anti-DriceAct (Yoo et al. 2002), rabbit anti-βGal (Cappel), mouse anti-Myc (Santa Cruz Biotechnology), rabbit anti-GFP (Clone Tech), and mouse anti-Arm (Jiang and Struhl 1998). Nuclear dye, 7-AAD, is from Molecular Probes.

Cell culture and immunoprecipitation

S2 cells were cultured in the Schneider's *Drosophila* Medium (Invitrogen) with 10% fetal bovine serum, 100 U/mL of penicillin, and 100 μg/mL of streptomycin. Transfection was carried out by using the Calcium Phosphate Transfection Kit (Specialty Media) according to manufacturer's instructions. To express dMST and Sav in S2 cells, corresponding UAS constructs were cotransfected with an ub-Gal4-expressing construct. Immunoprecipitation and Western blot analysis were performed by using standard protocols as previously described (Robbins et al. 1997). Antibodies used are mouse anti-Myc (Santa Cruz), mouse anti-HA, F7 (Santa Cruz), and mouse anti-Flag, M2 (Sigma).

Acknowledgments

We thank Jason Mercer, Maryam Shansab, and Brenda Fortney for conducting genetic screen, and Liping Luo for technical assistance. We thank Drs. Bruce Hay, Iswar Hariharan, H.D. Ryoo, Wei Du, and H. Richardson and the Bloomington stock center for reagents and fly stocks. J.J is supported by a grant from NIH, Searle Scholar Program from Chicago Trustee, Leukemia and Lymphoma Society Scholar Program, and Endowed Scholar Program in Biomedical Science from University of Texas Southwestern Medical Center.

The publication costs of this article were defrayed in part by payment of page charges. This article must therefore be hereby marked "advertisement" in accordance with 18 USC section 1734 solely to indicate this fact.

References

Abrams, J.M. 1999. An emerging blueprint for apoptosis in *Drosophila*. *Trends Cell. Biol.* **9:** 435–440.

Amanai, K. and Jiang, J. 2001. Distinct roles of central missing and dispatched in sending the Hedgehog signal. *Development* **128:** 5119–5127.

Basler, K. and Struhl, G. 1994. Compartment boundaries and the control of *Drosophila* limb pattern by *hedgehog* protein. *Nature* **368:** 208–214.

Cheung, W.L., Ajiro, K., Samejima, K., Kloc, M., Cheung, P., Mizzen, C.A., Beeser, A., Etkin, L.D., Chernoff, J., Earnshaw, W.C., et al. 2003. Apoptotic phosphorylation of histone H2B is mediated by mammalian sterile 20 kinase. *Cell* **113:** 507–517.

Creasy, C.L. and Chernoff, J. 1995a. Cloning and characterization of a human protein kinase with homology to Ste20. *J. Biol. Chem.* **270:** 21695–21700.

———. 1995b. Cloning and characterization of a member of the MST subfamily of Ste20-like kinases. *Gene* **167:** 303–306.

Creasy, C.L., Ambrose, D.M., and Chernoff, J. 1996. The Ste20-like protein kinase, Mst1, dimerizes and contains an inhibitory domain. *J. Biol. Chem.* **271:** 21049–21053.

Dan, I., Watanabe, N.M., and Kusumi, A. 2001. The Ste20 group kinases as regulators of MAP kinase cascades. *Trends Cell. Biol.* **11:** 220–230.

Freeman, M. 1996. Reiterative use of the EGF receptor triggers differentiation of all cell types in the *Drosophila* eye. *Cell* **87:** 651–660.

Glantschnig, H., Rodan, G.A., and Reszka, A.A. 2002. Mapping of MST1 kinase sites of phosphorylation: Activation and autophosphorylation. *J. Biol. Chem.* **277:** 42987–42996.

Graves, J.D., Gotoh, Y., Draves, K.E., Ambrose, D., Han, D.K., Wright, M., Chernoff, J., Clark, E.A., and Krebs, E.G. 1998. Caspase-mediated activation and induction of apoptosis by the mammalian Ste20-like kinase Mst1. *EMBO J.* **17:** 2224–2234.

Hanahan, D. and Weinberg, R.A. 2000. The hallmarks of cancer. *Cell* **100:** 57–70.

Hirai, S., Katoh, M., Terada, M., Kyriakis, J.M., Zon, L.I., Rana, A., Avruch, J., and Ohno, S. 1997. MST/MLK2, a member of the mixed lineage kinase family, directly phosphorylates and activates SEK1, an activator of c-Jun N-terminal kinase/stress-activated protein kinase. *J. Biol. Chem.* **272:** 15167–15173.

Jiang, J. and Struhl, G. 1995. Protein kinase A and Hedgehog signalling in *Drosophila* limb development. *Cell* **80:** 563–572.

———. 1998. Regulation of the Hedgehog and Wingless signalling pathways by the F-box/WD40-repeat protein Slimb. *Nature* **391:** 493–496.

Justice, R.W., Zilian, O., Woods, D.F., Noll, M., and Bryant, P.J. 1995. The *Drosophila* tumor suppressor gene warts encodes a homolog of human myotonic dystrophy kinase and is required for the control of cell shape and proliferation. *Genes & Dev.* **9:** 534–546.

Lee, K.K. and Yonehara, S. 2002. Phosphorylation and dimerization regulate nucleocytoplasmic shuttling of mammalian STE20-like kinase (MST). *J. Biol. Chem.* **277:** 12351–12358.

Lee, K.K., Murakawa, M., Nishida, E., Tsubuki, S., Kawashima, S., Sakamaki, K., and Yonehara, S. 1998. Proteolytic activation of MST/Krs, STE20-related protein kinase, by caspase during apoptosis. *Oncogene* **16:** 3029–3037.

Lee, K.K., Ohyama, T., Yajima, N., Tsubuki, S., and Yonehara, S. 2001. MST, a physiological caspase substrate, highly sensitizes apoptosis both upstream and downstream of caspase activation. *J. Biol. Chem.* **276:** 19276–19285.

Newsome, T.P., Asling, B., and Dickson, B.J. 2000. Analysis of *Drosophila* photoreceptor axon guidance in eye-specific mosaics. *Development* **127:** 851–860.

Richardson, H., O'Keefe, L.V., Marty, T., and Saint, R. 1995. Ectopic cyclin E expression induces premature entry into S phase and disrupts pattern formation in the *Drosophila* eye imaginal disc. *Development* **121:** 3371–3379.

Robbins, D.J., Nybakken, K.E., Kobayashi, R., Sisson, J.C., Bishop, J.M., and Therond, P.P. 1997. Hedgehog elicits signal transduction by means of a large complex containing the kinesin-related protein costal2. *Cell* **90:** 225–234.

Ryoo, H.D., Bergmann, A., Gonen, H., Ciechanover, A., and Steller, H. 2002. Regulation of *Drosophila* IAP1 degradation and apoptosis by reaper and ubcD1. *Nat. Cell. Biol.* **4:** 432–438.

St. John, M.A., Tao, W., Fei, X., Fukumoto, R., Carcangiu, M.L., Brownstein, D.G., Parlow, A.F., McGrath, J., and Xu, T. 1999. Mice deficient of Lats1 develop soft-tissue sarcomas, ovarian tumours and pituitary dysfunction. *Nat. Genet.* **21:** 182–186.

Stowers, R.S. and Schwarz, T.L. 1999. A genetic method for generating *Drosophila* eyes composed exclusively of mitotic clones of a single genotype. *Genetics* **152:** 1631–1639.

Tapon, N., Harvey, K.F., Bell, D.W., Wahrer, D.C., Schiripo, T.A., Haber, D.A., and Hariharan, I.K. 2002. *salvador* promotes both cell cycle exit and apoptosis in *Drosophila* and is mutated in human cancer cell lines. *Cell* **110:** 467–478.

Wolff, T. 2000. Histological techniques for the *Drosophila* eye. In Drosophila *protocols* (eds. W. Sullivan, et al.), pp. 201–272. Cold Spring Harbor Laboratory Press, Cold Spring Harbor, NY.

Wolff, T. and Ready, D.F. 1993. Pattern formation in the *Drosophila* retina. In *The development of* Drosophila melanogaster (eds. B. Bate and A. Martines Arias), pp. 1277–1325. Cold Spring Harbor Laboratory Press, Cold Spring Harbor, NY.

Xu, T., Wang, W., Zhang, S., Stewart, R.A., and Yu, W. 1995. Identifying tumor suppressors in genetic mosaics: The *Drosophila* lats gene encodes a putative protein kinase. *Development* **121:** 1053–1063.

Yoo, S.J., Huh, J.R., Muro, I., Yu, H., Wang, L., Wang, S.L., Feldman, R.M., Clem, R.J., Muller, H.A., and Hay, B.A. 2002. Hid, Rpr and Grim negatively regulate DIAP1 levels through distinct mechanisms. *Nat. Cell. Biol.* **4:** 416–424.